# Nano-structured interpenetrating composites with enhanced Young's modulus and desired Poisson's ratio

Hanxing Zhu [a,*], Tongxiang Fan [b], Chenghai Xu [c] and Di Zhang [b]

[a] School of Engineering, Cardiff University, Cardiff, CF24 3AA, UK

[b] State Key Lab of Metal Matrix Composites, Shanghai Jiaotong University, Shanghai, 200240, China

[c] Center for Composite Materials, Harbin Institute of Technology, Harbin, 150001, China

## Abstract

This paper has demonstrated that interpenetrating composites could be designed to not only have an significantly enhanced Young's modulus, but also have a Poisson's ratio at a desired value (e.g. positive, or negative, or zero). It is found that when the effect of the Poisson's ratio is absent, the Young's modulus of interpenetrating composites is closer to the Hashin and Shtrikman's upper limit than to their lower limit, and much larger than the simulation and experimentally measured results of the conventional isotropic particle or fibre composites. It is also illustrated that at the nanoscale, the interphase can either strengthen or weaken the stiffness, and the elastic properties of interpenetrating composites are size-dependent.

*Keywords*: A. Structural Composites; C. Elastic Properties; C. Modelling; B. Interphase.

## 1. Introduction

In nature, many living materials have an interpenetrating-phase structure, examples include fruits and vegetables which have a fibrous network embedded in a soft tissue. In an interpenetrating composite, if one constituent phase is damaged or removed, the remaining phase is a completely interconnected network and still has a good capacity to enable the mechanical function. Some people have produced interpenetrating composites and

---

experimentally measured their mechanical properties, and the interpenetrating phase structures have been found to significantly enhance the mechanical properties of the composites compared to the discontinuously reinforced phase structures [1-9]. Apart from enhancing the mechanical properties, the interpenetrating structure could also enable the best use of other functions of the constituent materials. For example, by using a correct constituent material, one penetrating phase could significantly enhance the thermal or electrical conductivity of the interpenetrating composite [10]. The available mechanics models and predictions for the conventional randomly distributed fibre or particle composites do not apply to their interpenetrating counterparts. Very little attempts have been made on analysing/modelling the mechanical properties of this type of composites [11-13], and it still remains unclear about how the detailed microstructures and the constituent materials of an interpenetrating composite affect its effective mechanical properties.

It has been found that the difference between the Poisson's ratios of the constituent materials could enhance the Young's modulus of a laminate material/composite [14, 15]. In addition, not only the Young's modulus of a composite could be much larger than the Voigt limit, but also the Poisson's ratio could be designed to have a desired value (e.g. positive, negative or zero) [16]. It has been generally recognised that for conventional particle or fibre composites at the nanometer scale, the smaller the filler (e.g. particles or fibres), the stiffer the composites [17-20]. In general, an interphase always exists between two different constituent materials in a composite, which can affect the mechanical properties of a composite due to two factors: interface adhesion and matrix crystalline structure [20, 21]. The effect of the former on the elastic properties of a composite is usually negligible because the elastic properties are associated to small deformation and not sensitive to small defects, while the latter could have a significant effect since the crystallinity of the matrix can remarkably increase the stiffness of the composite. The mechanical properties of the interphase are in general graded in the normal (i.e. thickness) direction. For a conventional composite, if the size of the filler is 100 *nm* or larger, the effects of the interphase/interface on the elastic properties of a composite are generally negligible [20, 22, 23].

This paper aims to study the combined effects of the constituent materials, the geometry and the size of the micro-structure on the effective elastic properties of interpenetrating composites, and particularly, to quantify how the elastic properties of an interpenetrating composite are affected by those of its constituent materials and by the size of the skeleton struts, and to design composites with a desired value of the Poisson's ratio. The obtained results may help to pave the way for the design of composites with enhanced/desired properties and interesting functions.

## 2. Geometrical Model

The interpenetrating composites are assumed to be made of two homogenous and isotropic constituent materials with Young's moduli $E_f$ and $E_m$, and Poisson's ratios $v_f$ and $v_m$. The filler is assumed to be a perfect open-cell foam with identical cubic cells, and the cell struts are assumed to have a length $2L$ and a uniform square cross-section of side $2t$. The matrix is the other part which completely fills the porous space of the skeleton/lattice filler (i.e. the open cell foam). The geometrical structure of this type of interpenetrating composites is periodic and made up by a large number of identical cubic unit cells. Figure 1 shows a representative volume element (RVE) of the composites, which is one-eighth of a periodic cubic unit cell. Obviously, the geometrical structure of the composites is symmetric to each of the six outside planes of the RVE. The volume fraction of the filler constituent material is

$$V_f = [3 \times (2t)^2 \times 2L - 2 \times (2t)^3]/(2L)^3 = \frac{3t^2}{L^2} - \frac{2t^3}{L^3} \tag{1}$$

and the volume fraction of the matrix constituent material is thus $V_m = 1 - V_f$.

The interphase between the filler and matrix in a composite is usually made up of a few layers of atoms and thus has a thickness $\tau$ between 1 and 5 $nm$, depending upon the combination of the two constituent materials and the manufacturing process. The elastic

properties of the interphase are usually graded in the thickness direction. For simplicity in the analysis and results, however, the interphase is assumed to have a uniform thickness $\tau$ and mean effective Young's modulus $E_i$ and mean Poisson's ratio $v_i$. The interphase may be formed completely from the original filler constituent, or completely from the original matrix constituent, or partly from the original filler and partly from the original matrix. The interphase thickness of a composite can be experimentally measured. Thus, the thickness $\tau$ is an intrinsic length dimension of a specific composite and thus can be used as a measure for the size-dependent effects at the nanometer scale.

## 3. Mechanics Model

As the structure of the interpenetrating composites, shown in Figure 1, has a cubic symmetry, the composites have only three independent elastic constants and are always almost isotropic. The interpenetrating composites contain three phases: filler, matrix, and a uniform interphase. In order to carry out theoretical analysis and obtain sufficient useful results, the mechanics model has to be simplified. Each of the front, top and right surfaces of the RVE is partitioned into nine rectangular areas, and the cubic RVE is partitioned into 27 blocks, as shown in Figure 2. To obtain the Young's modulus $E_{xx}$ and Poisson's ratio $v_{xy}$ for the interpenetrating composites, the cubic RVE is stretched to a strain $\varepsilon_x$ in the $x$ direction. According to the symmetry, the six outside planes of the RVE remain plane after deformation, and the normal stresses on the nine rectangular areas of the top surface are exactly the same as those on the right surface. For simplicity, we consider only the normal stresses within the blocks of the RVE, and ignore the shear stresses and the compatibility conditions between the blocks inside the RVE. The normal stresses in each of the 27 blocks are further assumed to be uniform, as shown in Figure 2, thus they have constant values to be determined. To obtain the solution, the back, left and bottom surfaces of the RVE are restrained in their normal directions, the front surface is imposed a displacement $L\varepsilon_x$ in the $x$

direction, and the top and right surfaces are imposed the same amplitude of displacement $L\varepsilon_y$

in their normal directions ($\varepsilon_y$ is an unknown to be determined). Using Hooke's law and the

deformation compatibility conditions of the outside planes of the RVE, we have following

equations:

$$\frac{t}{E_f}(\sigma_{x1}-2v_f\sigma_{y1})+\frac{\tau}{E_f}(\sigma_{x1}-2v_f\sigma_{y2})+\frac{L-t-\tau}{E_f}(\sigma_{x1}-2v_f\sigma_{y3})=L\varepsilon_x \tag{2}$$

$$\frac{t}{E_f}(\sigma_{x2}-v_f\sigma_{y1}-v_f\sigma_{y4})+\frac{\tau}{E_i}(\sigma_{x2}-v_i\sigma_{y2}-v_i\sigma_{y5})+\frac{L-t-\tau}{E_i}(\sigma_{x2}-v_i\sigma_{y3}-v_i\sigma_{y6})=L\varepsilon_x \tag{3}$$

$$\frac{t}{E_f}(\sigma_{x3}-v_f\sigma_{y1}-v_f\sigma_{y7})+\frac{\tau}{E_i}(\sigma_{x3}-v_i\sigma_{y2}-v_i\sigma_{y8})+\frac{L-t-\tau}{E_m}(\sigma_{x3}-v_m\sigma_{y3}-v_m\sigma_{y9})=L\varepsilon_x \tag{4}$$

$$\frac{t}{E_i}(\sigma_{x4}-2v_i\sigma_{y4})+\frac{\tau}{E_i}(\sigma_{x4}-2v_i\sigma_{y5})+\frac{L-t-\tau}{E_i}(\sigma_{x4}-2v_i\sigma_{y6})=L\varepsilon_x \tag{5}$$

$$\frac{t}{E_i}(\sigma_{x5}-v_i\sigma_{y4}-v_i\sigma_{y7})+\frac{\tau}{E_i}(\sigma_{x5}-v_i\sigma_{y5}-v_i\sigma_{y8})+\frac{L-t-\tau}{E_m}(\sigma_{x5}-v_m\sigma_{y6}-v_m\sigma_{y9})=L\varepsilon_x \tag{6}$$

$$\frac{t}{E_m}(\sigma_{x6}-2v_m\sigma_{y7})+\frac{\tau}{E_m}(\sigma_{x6}-2v_m\sigma_{y8})+\frac{L-t-\tau}{E_m}(\sigma_{x6}-2v_m\sigma_{y9})=L\varepsilon_x \tag{7}$$

$$\frac{t}{E_f}(\sigma_{y1}-v_f\sigma_{x1}-v_f\sigma_{y1})+\frac{\tau}{E_f}(\sigma_{y1}-v_f\sigma_{x2}-v_f\sigma_{y4})+\frac{L-t-\tau}{E_f}(\sigma_{y1}-v_f\sigma_{x3}-v_f\sigma_{y7})=L\varepsilon_y \tag{8}$$

$$\frac{t}{E_f}(\sigma_{y2}-v_f\sigma_{x1}-v_f\sigma_{y2})+\frac{\tau}{E_i}(\sigma_{y2}-v_i\sigma_{x2}-v_i\sigma_{y5})+\frac{L-t-\tau}{E_i}(\sigma_{y2}-v_i\sigma_{x3}-v_i\sigma_{y8})=L\varepsilon_y \tag{9}$$

$$\frac{t}{E_f}(\sigma_{y3}-v_f\sigma_{x1}-v_f\sigma_{y3})+\frac{\tau}{E_i}(\sigma_{y3}-v_i\sigma_{x2}-v_i\sigma_{y6})+\frac{L-t-\tau}{E_m}(\sigma_{y3}-v_m\sigma_{x3}-v_m\sigma_{y9})=L\varepsilon_y \tag{10}$$

$$\frac{t}{E_f}(\sigma_{y4} - v_f\sigma_{x2} - v_f\sigma_{y1}) + \frac{\tau}{E_i}(\sigma_{y4} - v_i\sigma_{x4} - v_i\sigma_{y4}) + \frac{L-t-\tau}{E_i}(\sigma_{y4} - v_i\sigma_{x5} - v_i\sigma_{y7}) = L\varepsilon_y \qquad (11)$$

$$\frac{t}{E_i}(\sigma_{y5} - v_i\sigma_{x2} - v_i\sigma_{y2}) + \frac{\tau}{E_i}(\sigma_{y5} - v_i\sigma_{x4} - v_i\sigma_{y5}) + \frac{L-t-\tau}{E_i}(\sigma_{y5} - v_i\sigma_{x5} - v_i\sigma_{y8}) = L\varepsilon_y \qquad (12)$$

$$\frac{t}{E_i}(\sigma_{y6} - v_i\sigma_{x2} - v_i\sigma_{y3}) + \frac{\tau}{E_i}(\sigma_{y6} - v_i\sigma_{x4} - v_i\sigma_{y6}) + \frac{L-t-\tau}{E_m}(\sigma_{y6} - v_m\sigma_{x5} - v_m\sigma_{y9}) = L\varepsilon_y \qquad (13)$$

$$\frac{t}{E_f}(\sigma_{y7} - v_f\sigma_{x3} - v_f\sigma_{y1}) + \frac{\tau}{E_i}(\sigma_{y7} - v_i\sigma_{x5} - v_i\sigma_{y4}) + \frac{L-t-\tau}{E_m}(\sigma_{y7} - v_m\sigma_{x6} - v_m\sigma_{y7}) = L\varepsilon_y \qquad (14)$$

$$\frac{t}{E_i}(\sigma_{y8} - v_i\sigma_{x3} - v_i\sigma_{y2}) + \frac{\tau}{E_i}(\sigma_{y8} - v_i\sigma_{x5} - v_i\sigma_{y5}) + \frac{L-t-\tau}{E_m}(\sigma_{y8} - v_m\sigma_{x6} - v_m\sigma_{y8}) = L\varepsilon_y \qquad (15)$$

$$\frac{t}{E_m}(\sigma_{y9} - v_m\sigma_{x3} - v_m\sigma_{y3}) + \frac{\tau}{E_m}(\sigma_{y9} - v_m\sigma_{x5} - v_m\sigma_{y6}) + \frac{L-t-\tau}{E_m}(\sigma_{y9} - v_m\sigma_{x6} - v_m\sigma_{y9}) = L\varepsilon_y \qquad (16)$$

In addition, the total force on the top or right surface of the RVE must vanish for uniaxial tension, leading to

$$t^2\sigma_{y1} + t\tau\sigma_{y2} + t(L-t-\tau)\sigma_{y3} + t\tau\sigma_{y4} + \tau^2\sigma_{y5} + (L-t-\tau)\tau\sigma_{y6}$$

$$+(L-t-\tau)t\sigma_{y7} + (L-t-\tau)\tau\sigma_{y8} + (L-t-\tau)^2\sigma_{y9} \qquad (17)$$

Thus, the 16 unknowns, $\sigma_{x1}$, $\sigma_{x2}$, $\sigma_{x3}$, $\sigma_{x4}$, $\sigma_{x5}$, $\sigma_{x6}$, $\sigma_{y1}$, $\sigma_{y2}$, $\sigma_{y3}$, $\sigma_{y4}$, $\sigma_{y5}$, $\sigma_{y6}$, $\sigma_{y7}$, $\sigma_{y8}$, $\sigma_{y9}$ and $\varepsilon_y$, can be fully determined from the 16 simultaneous linear Equations (2) to (17). The effective stress of the interpenetrating composites in the x direction is defined as

$$\sigma_x = [t^2\sigma_{x1} + 2t\tau\sigma_{x2} + 2t(L-t-\tau)\sigma_{x3} + \tau^2\sigma_{x4} + 2(L-t-\tau)\tau\sigma_{x5} + (L-t-\tau)^2\sigma_{x6}]/L^2 \qquad (18)$$

The Young's modulus and Poisson's ratio of the interpenetrating composites can thus be obtained as

$$E_{xx} = \frac{\sigma_x}{\varepsilon_x} \tag{19}$$

$$v_{xy} = -\frac{\varepsilon_y}{\varepsilon_x} \tag{20}$$

## 4. Results

The mechanics model of the three-phase composites presented in section 3 remains correct for the two-phase interpenetrating composites when the effects of the interphase are absent (i.e. when the thickness of the interphase $\tau$ is much smaller than the size of the filler $t$, or tends to 0). In the following, we will first present the elastic properties of the interpenetrating composites when the effects of the interphase are absent, then explore how to make the Young's modulus of the composites greater than the Voigt limit and the Poisson's ratio at a desired value, and finally investigate the size-dependent effects of the interphase on the elastic properties of the nano-sized interpenetrating composites.

Figures 3(a) -(c) show the effects of the volume fraction of the filler constituent on the Young's modulus of the interpenetrating composites with the interphase thickness $\tau = 0$ (or $\tau \ll t$). The Voigt and Reuss limits, and the Hashin and Shtrikman's upper and lower bounds [24] are also included for comparison, and all the results are normalised by the Voigt limit $(E_C)_V = E_f V_f + E_m V_m$. When the effect of the Poisson ratios of the filler and matrix constituents is minimised by setting $v_f = v_m = 0.3$, the larger the ratio of $E_f / E_m$, the larger the differences among the Young's modulus of the interpenetrating composites and the different upper and lower limits, as can be seen by comparing Fig. 3(a) to Fig. 3(b). If $E_f / E_m = 1.0$ and $v_f = v_m$, the two-phase interpenetrating composites would become a single material (in the mechanics point of view) and the results given by all different upper and

lower limits would be the same. When $E_f / E_m = 2.0$, $v_f = 0.05$, and $v_m = 0.495$, Fig. 3(c) demonstrates that the Young's modulus of the interpenetrating composites is constantly larger than the Voigt limit, indicating that the difference between the Poisson's ratios of the constituent materials can significantly enhance the stiffness of the composites. The Poisson's ratio of isotropic materials can span from -1.0 to 0.5, i.e. $-1.0 < v < 0.5$ [25--27]. For example, solid polymer or rubber materials, or low density regular BCC and random irregular open cell foams [26, 27] have a Poisson's ratio very close to 0.5; most metal materials have a Poisson's ratio between 0.1 and 0.4; cork has a Poisson's ratio close to zero [28]; auxetic foams can have an isotropic Poisson's ratio close to -1.0 [29].

When the effect of the interphase is absent (i.e. $\tau = 0$ or $\tau << t$), Figures 4(a, b) and 5(a, b) illustrate the effects of different combinations between the Young's moduli and Poisson's ratios of the filler and matrix constituents on the effective Young's modulus and Poisson's ratio of the interpenetrating composites, where the Young's modulus of the composites is normalized by $(E_C)_V = E_f V_f + E_m V_m$. As can be seen from Figures 4(a) and 4(b), the Young's modulus of the interpenetrating composites can be made much larger than the Voigt limit. The larger the difference between the Poisson's ratios of the constituent materials, the larger the dimensionless effective Young's modulus of the composites; and the larger the difference between the Young's moduli of the filler and matrix constituent materials, the smaller the dimensionless effective Young's modulus of the composites. Figures 5(a) and 5(b) demonstrate that the Poisson's ratio of an interpenetrating composite can be designed to have a desired value, e.g. positive, negative or zero, depending upon the requirement for specific application. These results provide a guide for us to design and produce interesting and useful functional materials/structures for different applications. For example, materials with a zero Poisson's ratio are ideal for sealing applications [28].

The interphase could occur either in the original filler, or in the original matrix, or in both of them, depending upon the combination of the two constituent materials and the manufacturing process. For composites made of constituent materials with $E_f = 2.0 E_m$,

$v_f = 0.05$ and $v_m = 0.495$, Figures 6(a) – 6(d) present the size-dependent relationships between the effective Young's modulus and the volume fraction of the original filler $V_f$, where the Young's modulus has been normalised by the Voigt limit. The interphase thickness $\tau$ has a fixed value between 1 and 5 nm. When the ratio of $\tau / t$ is close to 1.0, the actual size of the filler skeleton/lattice is very small (It is noted that the thickness of the filler is *2t*); when the ratio of $\tau / t$ tends to 0, the actual size of the filler is much larger than thickness of the interphase. When the interphase is completely formed from the original matrix constituent material and if $E_i = E_f$ and $v_i = v_f$, the size-dependent relationships between the Young's modulus of the interpenetrating composites and the volume fraction of the original filler constituent material are illustrated in Figure 6(a). When the filler is much larger than the interphase thickness (i.e. $\tau / t = 0.0$), the interphase has no effect on the Young's modulus of the interpenetrating composites, and the results reduce to the curve shown in Fig. 4 (a). The dimensionless Young's modulus of the composites is still larger than 1.0 due to effect of the big difference between the Poisson's ratios of the two constituent materials. When the size of the filler is very small (e.g. $\tau / t = 1.0$), the interphase can significantly enhance the Young's modulus of the interpenetrating composites. When $\tau / t = 0.1$, the contribution of the interphase to the Young's modulus of the composites is about 5%. This is consistent with the finding for isotropic particle composites [22, 30]. In theoretical analyses, the interface/interphase was often assumed to have a zero thickness (i.e. $\tau = 0$, the volume of the interphase was treated as zero in some theoretical analyses) and a non-zero (positive or negative) surface/interface modulus with an amplitude of a few *N/m*. Thus, it would be very straightforward that when the interface modulus ($S = \tau E_i$) is positive, the smaller the particles, the larger the total interface area (for the same volume fraction of the filler) and thus the stiffer the composites. The effect on the Young's modulus is reversed if the interface modulus is negative. When the interphase is completely formed from the original filler constituent and if $E_i = E_m$ and $v_i = v_m$, the size-dependent relationships between the Young's modulus of the interpenetrating composites and the volume fraction of the original filler are demonstrated in Figure 6(b). In this case, the smaller the filler, the smaller the dimensionless Young's

modulus of the composites.   When the interphase is formed half from the original filler and half from the original matrix, and if $E_i = E_m$ and $v_i = v_m$, the size-dependent relationships between the Young's modulus of the interpenetrating composites and the volume fraction of the original filler are plotted in Figure 6(c).   In this case, the smaller the filler, the smaller the dimensionless Young's modulus of the composites.   When the interphase is formed half from the original filler and half from the original matrix, and if $E_i = E_f$ and $v_i = v_f$, the size-dependent relationships between the Young's modulus of the composites and the volume fraction of the original filler are presented in Figure 6(d).   In this case, the smaller the filler, the larger the dimensionless Young's modulus of the composites.

## 5. Discussion

To validate the analytical results for the effective Young's moduli and Poisson's ratios obtained in the above section, the RVE of the interpenetrating composites was partitioned into 8000 C3D8 elements and the ABAQUS software was used to perform a number of simulations (i.e. numerical experiments). Table 1 shows a comparison between the analytical results and the FEA simulation results, where the effective Young's moduli of the composites have been normalized by the Voigt limit.   As can be seen, the analytical results for the Young's modulus of the interpenetrating composites obtained from Equations (2) – (20) are constantly smaller than the simulation results, indicating that the analytical results always underestimate the Young's modulus of the composites. This is consistent with the mechanics principle because the restraints inside the RVE in the finite element analysis are much stronger than those in the simplified analytical model, and any additional restraint always tends to make a material or structure stiffer [16].

For the case when $v_f = 0.05$, $v_m = -0.495$ and $\tau = 0$, and another case when $v_f = 0.45$, $v_m = -0.8$, $\tau = t$, and the interphase is assumed to be completely formed from the original matrix constituent, the differences between the analytical results of the Young's modulus and Poisson's ratio of the interpenetrating composites obtained from Eqs (2) – (20) and those

obtained from the ABAQUS simulations are less than 5%, suggesting that the simplified analytical model is quite accurate.   For the other two cases when $v_f = 0.45$, $v_m = -0.8$ and $\tau = 0$, the Young's moduli obtained from the ABAQUS simulations are significantly larger than the analytical results.   This is because the deformed blocks may have been significantly distorted, and hence the simplified analytical model may have strongly violated the compatibility conditions between the divided blocks inside the RVE.   Obviously, if $E_f = E_m$ and $v_f = v_m$, the analytical results would be exactly the same as the finite element simulation results; the larger the differences between the elastic properties of the filler and matrix constituents, the more the analytical model tends to underestimate the Young's modulus of the interpenetrating composites.   Nevertheless, as can be seen from table 1, the predicted results are very accurate for all the cases when both the filler and matrix constituent materials have a positive Poisson's ratio.

One primary objective of this paper is to demonstrate that interpenetrating composites have a much larger Young's modulus than that of their conventional isotropic particle or fibre counterparts.   To this aim, we compare the Young's moduli of the interpenetrating composites to some published experimentally measured results [31-33] and simulation results [34-36] of isotropic particle or fibre composites.   Table 2 shows the elastic properties of the constituent materials of the conventional isotropic particle or fibre composites in the experiments [31-33] and simulations [34-36].   Figures 7(a) and 7(b) present a comparison of the Young's moduli of the interpenetrating composites to the experimental results and the simulation results, where all the Young's moduli are normalised by the Hashin and Shtrikman's upper limit.   It is noted that to directly compare the normalised Young's moduli of the interpenetrating composites to those of the particle or fibre composites [31-36] in Figures 7(a) and 7(b), the same values $v_f = v_m = 0.3$ and different actual values of $E_f / E_m$ were used to obtain the results for interpenetrating composites with different values of the filler volume fraction given in [31-36].   For example, in order to directly compare the experimental results of Sic/Al particle composites [31] in Figure 7(a), the ratio

$E_f / E_m = 410 / 74 = 5.54$ (see table 2) and values $v_f = v_m = 0.3$ were used to obtain the normalised Young's moduli of interpenetrating composites with different values of filler volume fraction: $V_f = 0.1$, 0.2 and 0.3. At values of filler volume fraction when there is no experimental or simulation result available for a direct comparison, the normalised Young's moduli of interpenetrating composites in Figures 7(a) and 7(b) were obtained on the assumptions that $E_f / E_m = 10$ and $v_f = v_m = 0.3$. As can be seen in Figures 7(a) and 7(b), the value of the normalised Young's modulus of interpenetrating composite swings away from a 'supposed' smooth curve at some different values of $V_f$. This is because different values of $E_f / E_m$ (see table 2) were used to obtain the normalised Young's moduli for the interpenetrating composites.

It is noted that the smaller the ratio of $E_f / E_m$, the relatively smaller would be the difference between the Young's modulus of the interpenetrating composite and the Hashin and Shtrikman's upper limit, as can be seen from Figures 3a and 3b, and consequently the larger would be the normalised Young's modulus of the interpenetrating composite. As the effect of the Poisson's ratios exists in the experimental results [31-33] and in the simulation results [34-36], we could conclude that the interpenetrating composites always have a much larger Young's modulus than their conventional isotropic particle or fibre counterparts.

## 6. Conclusions

Based on the results obtained in this paper, following conclusions can be drawn:

(1) Interpenetrating composites could have a Young's modulus much greater than the Voigt limit. In general, the larger the difference between the Poisson's ratios of the two constituent materials, the larger the Young's modulus of the composites.

(2) The Young's modulus of interpenetrating composites is closer to the Hashin and Shtrikman's upper limit than to their lower limit, and much larger than the experimental and simulation results of the conventional isotropic particle or fibre composites.

(3) Interpenetrating composites could have a desired value of the Poisson's ratio, e.g. positive, negative, or zero, and thus could have many interesting and important applications, e.g. functional materials/structures.

(4) The interphase could either stiffen or weaken an interpenetrating composite when the filler size is at the nanometer scale, depending upon the combination of the two constituent materials and the manufacturing process. The size-dependent effects vanish when the size of the filler/particle is much larger than interphase thickness (e.g. $t \geq 20\tau$).

## References

[1] Clark DR. Interpenetrating phase composites. J Am Ceram Soc 1992; 75: 739-759.

[2] Breslin MC, Ringnalda J, Xu L, Fuller M, Seeger J, Daehn GS, Otani T, Fraaser HL. Processing, microstructure, and properties of co-continuous aluminia-aluminum Composites. Mater Sci Eng A 1995; 195: 113-119.

[3] Ravichandran KS. Deformation behaviour of interpenetrating phase composites. Compos Sci Tech 1994; 52: 541-549.

[4] Peng HX, Fan Z, Evans JRG. Bi-continuous metal matrix composites. Mater Sci Eng A 2001; 303: 37-45.

[5] Marchi CS, Kouzeli M, Rao R, Lewis JA, Dunand DC. Alumina-aluminum interpenetrating-phase periodic architecture. Scrpta Mater 2003; 49: 861-866.

[6] Mattern A, Huchler B, Staudenecker D, Oberacker R, Nagel A, Hoffmann MJ. Preparation of interpenetrating ceramic-metal composites. J European Ceram Soc 2004; 24: 3399-3408.

[7] Moon RJ, Tilbrook M, Hoffman M, Al-Al$_2$O$_3$ composites with interpenetrating network structures: composite modulus estimation. J Am Ceram Soc 2005; 88: 666-674.

[8] Tilbrook MT, Moon RJ, Hoffman M. On the mechanical properties of alumina-epoxy composites with an interpenetrating network structure. Mater Sci Eng A 2005; 393: 170-178.

[9] Huang LJ, Geng L, Peng HX, Balasubramaniam K, Wang GS. Effects of sintering parameters on the microstructure and tensile properties of in situ TiBw/Ti6Al4V composites with a novel network architecture. Mater Design 2011; 32: 3347-3353.

[10] Zhu HX, Fan TX, Zhang D. Composite materials with enhanced conductivities. Adv Eng Mater 2016; 18: 1174-1180.

[11] Lessle P, Dong M, Schmauder S. Self-consistent matricity model to simulate the mechanical behaviour of interpenetrating microstructures. Comput Mater Sci 1999; 15: 455-465.

[12] Wegner LD, Gibson LJ. The mechanical behaviour of interpenetrating phase composites – I: modelling. Int J Mech Sci 2000; 42: 925-942.

[13] Feng XQ, Tian Z, Liu YH, Yu SW. Effective elastic and plastic properties of interpenetrating multiphase composites. Appl Compos Mater 2004; 11: 33-55.

[14] Lim TC. Out-of-plane modulus semi-auxetic laminates. European J Mech A/Solids 2009; 28: 752-756.

[15] Liu B, Feng X, Zhang SM. The effective Young's modulus of composites beyond the Voigt estimate due to the Poisson effect. Compos Sci Tech 2009; 69: 2198-2204.

[16] Zhu HX, Fan TX, Zhang D. Composite materials with enhanced dimensionless Young's modulus and desired Poisson's ratio. Scientific Reports 2015; 5: 14103.

[17] Ji XL, Jing JK, Jiang BZ. Tensile modulus of polymer nanocomposites. Poly Eng Sci 2002; 42: 983-993.

[18] Dounce J, Boilot JP, Biteau J, Scodellaro L, Jimenez A. Effect of filler size and surface condition of nano-sized silica particles in polysiloxane coatings. Thin Solid Films 2004; 466: 114-122.

[19] Mishra S, Sonawane SH, Singh RP. Studies on characterization of nano CaCO3 prepared by the in situ deposition technique and its application in PP-nano CaCO3 composites. J Polym Sci Part B Polym Phys 2005; 43: 107-113.

[20] Fu SY, Feng XQ, Leuke B, Mai YW. Effects of particle size, particle/matrix interface

adhesion and particle loading on mechanical properties of particulate-polymer composites. Composites Part B 2008; 39: 933-961.

[21] Wang K, Wu J, Ye L, Zeng H. Mechanical properties and toughening mechanisms of polypropylene/barium sulfate composites. Composite Part A 2003; 34: 1199-1205.

[22] Duan HL, Wang J, Huang ZP, Karihaloo BL. Size-dependent effective elastic constants of solids containing nano-inhomogeneities with interface stress. J Mech Phys Solids 2005; 53: 1574-1596.

[23] Shabana YM, Karihaloo BL, Zhu HX, Kulasegaram S. Influence of processing defects on the measured properties of Cu-Al2O3 composites: A forensic investigation. Compos Part A 2013; 46:140-146.

[24] Hashin Z, Shtrikman S. A variational approach to the theory of the elastic behaviour of multiphase materials. J Mech Phys Solids 1963; 11: 127-140.

[25] Lakes RS. Foam structures with a negative Poisson's ratio. Science 1987; 235: 1038-1040.

[26] Zhu HX, Knott JF, Mills NJ. Analysis of the elastic properties of open-cell foams with tetrakaidecaheral cells. J Mech Phys Solids 1997; 45: 319-343.

[27] Zhu HX, Hobdell RJ, Windle AH. Effects of cell irregularity on the elastic properties of open cell foams. Acta Materialia 2000; 48: 4893-4900.

[28] Gibson LJ, Ashby MF. Cellular Solids – Structures and Properties. Cambridge University Press, UK; 1997.

[29] Milton GM. Composite materials with Poisson's ratio close to -1. J Mech Phys Solids 2992; 40: 1105-1137.

[30] Duan HL, Wang J, Huang ZP, Zhong Y. Stress fields of a spheroidal inhomogeneity with an interphase in an infinite medium under remote loading. Proc Roy Soc A 2005; 461: 1055-1080.

[31] Chawla N, Sidhu RS, Ganesh VV. Three-dimensional visualization and microstructure-based modelling of deformation in particle-reinforced composites. Acta Mater 2006; 54: 1541-1548.

[32] Dekkers MEJ, Heikens D. The effects of interfacial adhesion on the tensile behavior of polystyrene-Glass-Bead composites. J Appl Polym Sci 1983; 28: 3809-3815.

[33] Rousseau CE, Tippur HV. Compositionally graded materials with cracks normal
to the elastic gradient.    Acta Mater 2000; 48: 4021-4033.

[34] Hua Y, Gu L. Prediction of the thermomechanical behavior of particle-reinforced metal
matrix composites. Composites Part B    2013; 45: 1464-1470.

[35] Kari S, Berger H, Reinaldo-Ramos R, Gabbert U. Computational evaluation of
effective material properties of composites reinforced by randomly distributed spherical
particles. Composite Structures 2007; 77: 223-231.

[36] Marur PR, Estimation of effective elastic properties and interface stress concentrations
in particulate composites by unit cell methods.    Acta Mater 2004; 52: 1263-1270.

Table 1.   Comparison between the analytical results and finite element simulation results

| Composite Material | Analytical Results | | Simulation Results | |
|---|---|---|---|---|
| | $E_{xx}/(E_C)_{upper}$ | $v_{xy}$ | $E_{xx}/(E_C)_{upper}$ | $v_{xy}$ |
| $E_f = 2E_m$   $V_f = 0.104$<br>$v_f = 0.05$   $v_m = 0.495$<br>$\tau = 0.0$ | 1.0088 | 0.4782 | 1.0281 | 0.48042 |
| $E_f = 2E_m$   $V_f = 0.50$<br>$v_f = 0.05$   $v_m = 0.495$<br>$\tau = 0.0$ | 1.0536 | 0.3609 | 1.1033 | 0.3731 |
| $E_f = 2E_m$   $V_f = 0.104$<br>$v_f = 0.45$   $v_m = -0.8$<br>$\tau = 0.0$ | 1.1704 | -0.6979 | 1.8315 | -0.5391 |
| $E_f = 2E_m$   $V_f = 0.50$<br>$v_f = 0.45$   $v_m = -0.8$<br>$\tau = 0.0$ | 1.5321 | -0.0846 | 2.054 | -0.1355 |
| $E_f = 2E_m$   $V_f = 0.104$<br>$v_f = 0.45$   $v_m = -0.8$<br>$\tau = t$, $E_i = 1.5E_m$, $v_i = -0.175$ | 1.1270 | 0.3899 | 1.1431 | 0.3913 |

Table 2. Elastic properties of the constituent materials in experiments [31-33] and simulations [34-36]

| Composites | $E_f$ (GPa) | $v_f$ | $E_m$ (GPa) | $v_m$ |
|---|---|---|---|---|
| SiC_particle/Al [31] | 410 | 0.19 | 74 | 0.33 |
| Glass_particle/Polystyrene [32] | 70 | 0.22 | 3.25 | 0.34 |
| Glass/Epoxy [33] | 69 | 0.15 | 3.0 | 0.35 |
| SiC_fibre/Al [34] | 410 | 0.19 | 74 | 0.33 |
| Particle/matrix [35] | 450 | 0.17 | 70 | 0.3 |
| Glass_particle/Epoxy [36] | 69 | 0.15 | 3.0 | 0.35 |

# Figures
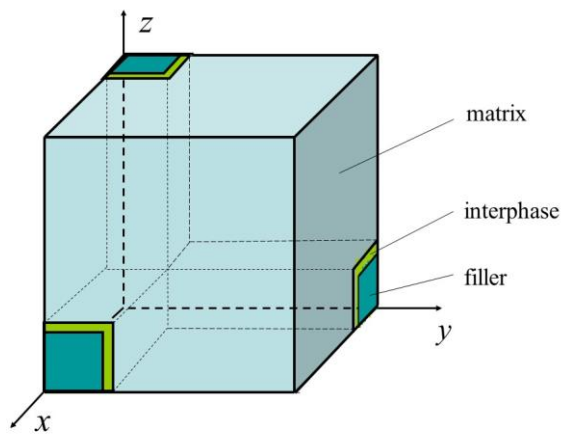


Fig. 1.    A representative volume element (RVE).
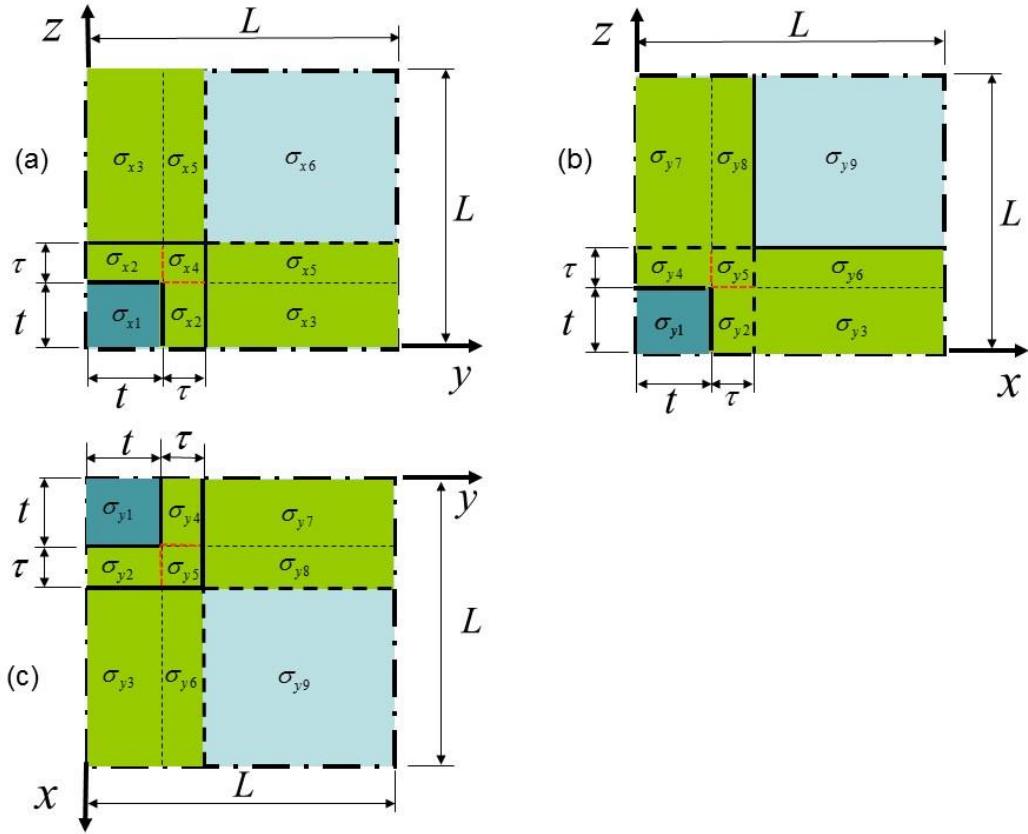
Fig. 2.   Mechanics model of the RVE.
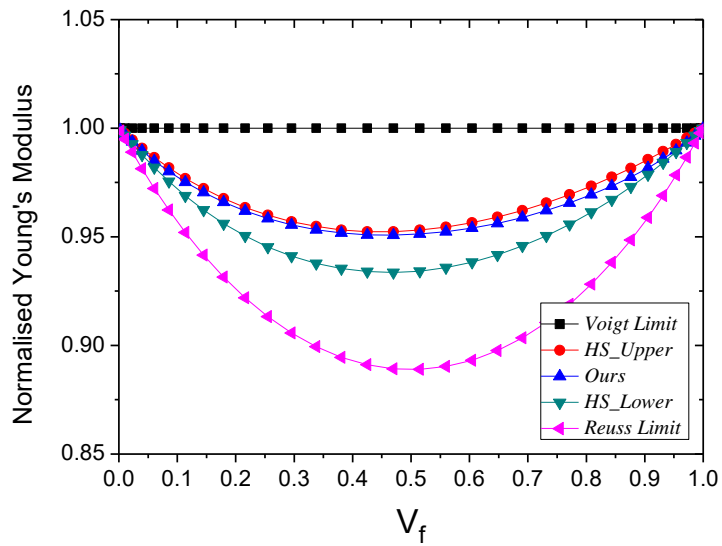


(a)
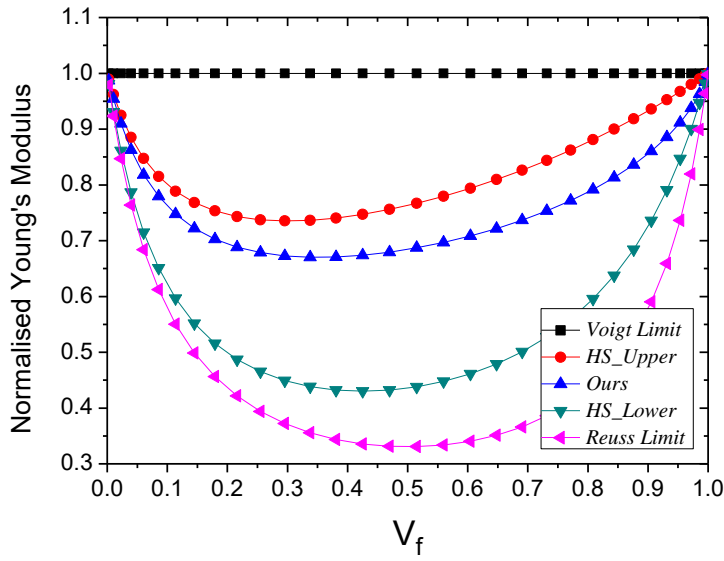
(b)
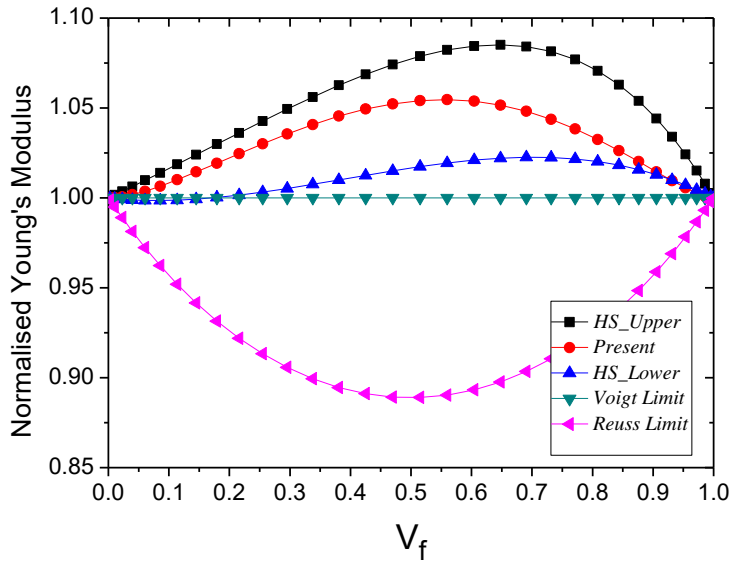


(c)

Figure 3. Effects of filler volume fraction on the Young's modulus of interpenetrating composites when the interphase thickness tends to zero (or $\tau \ll t$). The Young's modulus is normalised by the Voigt limit, and different upper and lower limits are also included for comparison. (a) $E_f = 2.0E_m$, $v_f = v_m = 0.3$, (b) $E_f = 10.0E_m$, $v_f = v_m = 0.3$, (c) $E_f = 2.0E_m$, $v_f = 0.05$, $v_m = 0.495$.
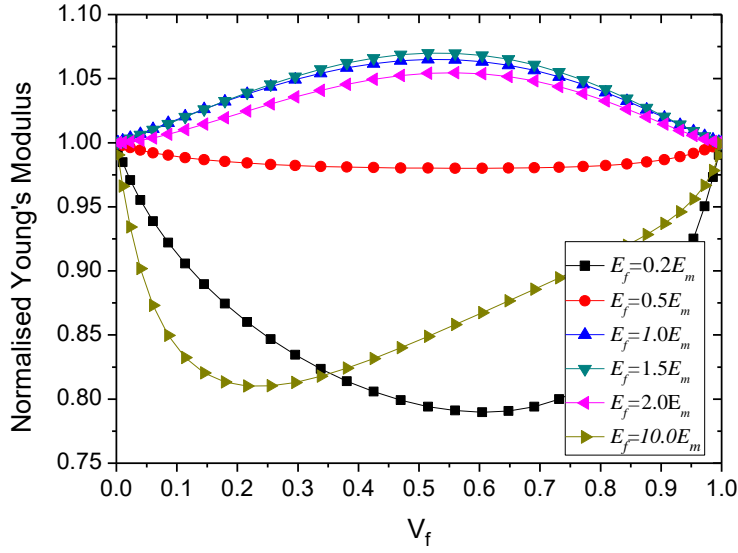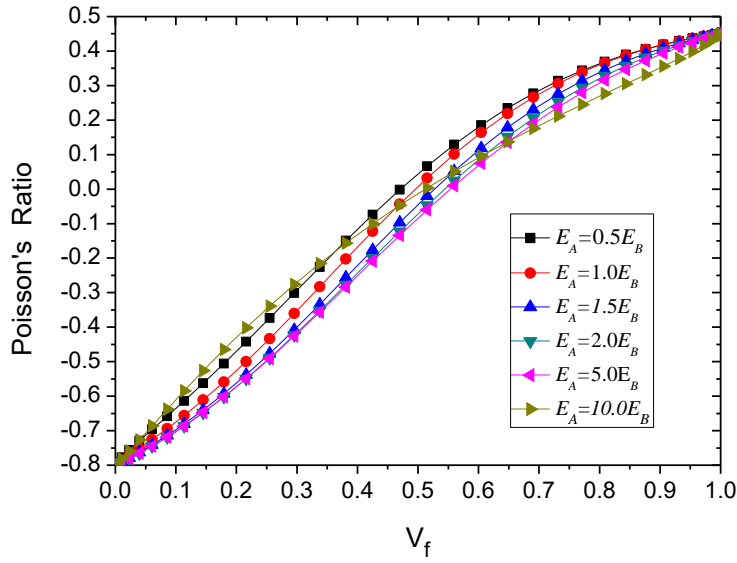
(a)
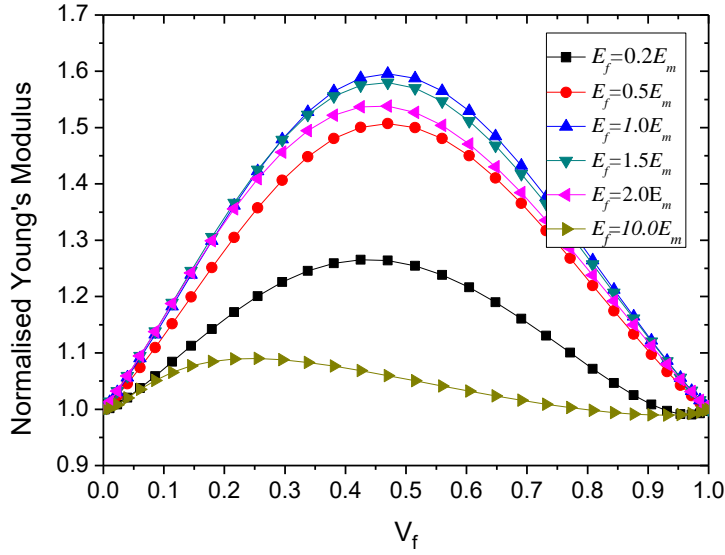


(b)

Figure 4. Effects of the ratio of $E_f / E_m$ on the dimensionless Young's modulus of interpenetrating composites when the interphase thickness tends to zero (or $\tau << t$). (a) $v_f = 0.05$ and $v_m = 0.495$; (b) $v_f = 0.45$ and $v_m = -0.8$.
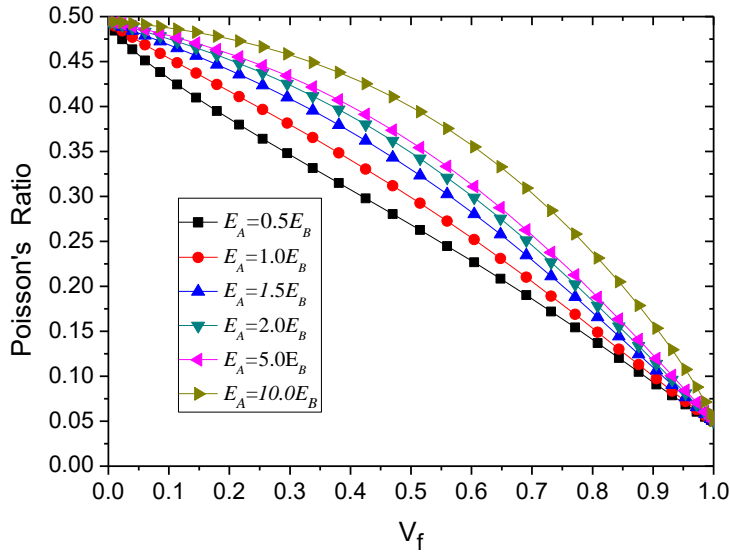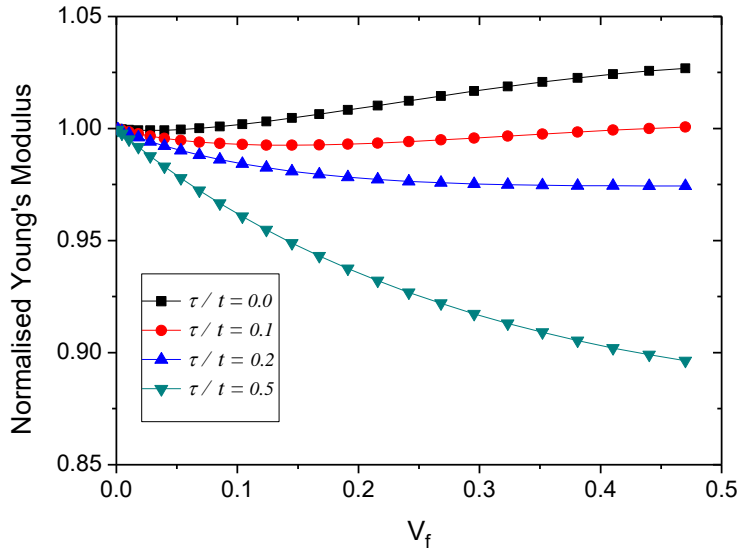
(a)



(b)

Figure 5. Effects of the ratio of $E_f / E_m$ on the Poisson's ratio of interpenetrating composites when the interphase thickness tends to zero (or $\tau << t$). (a) $v_f = 0.05$ and $v_m = 0.495$; (b) $v_f = 0.45$ and $v_m = -0.8$.
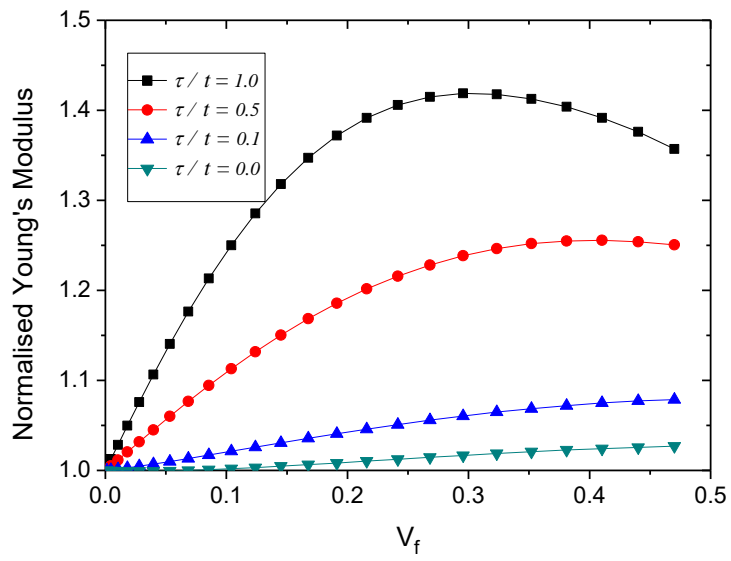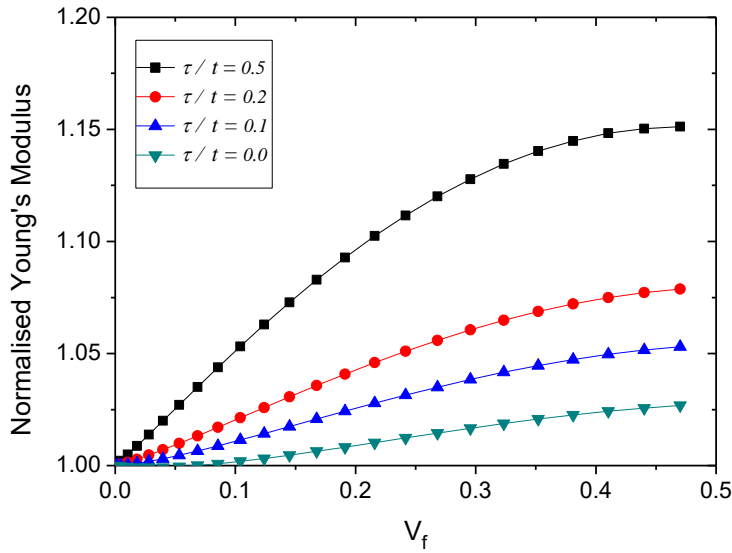
(a)
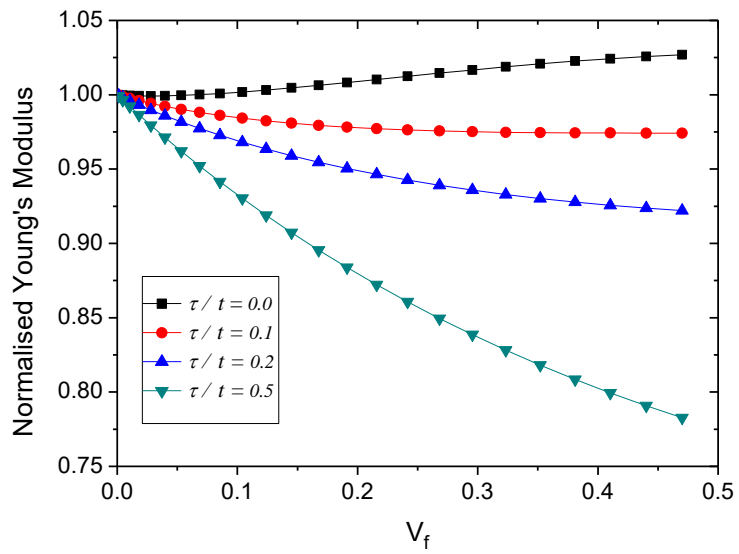


(b)

(c)



(d)

Figure 6. Size-dependent relations between the dimensionless Young's modulus and the filler volume fraction when $E_f = 2.0E_m$, $v_f = 0.05$, $v_m = 0.495$. (a) Interphase is formed from the matrix and $E_i = E_f$ and $v_i = v_f$; (b) Interphase is formed from the filler and $E_i = E_m$ and $v_i = v_m$; (c) Interphase is formed half from the filler and half from the matrix, and $E_i = E_m$ and $v_i = v_m$; (d) Interphase is formed half from the filler and half from the matrix, $E_i = E_f$ and $v_i = v_f$.
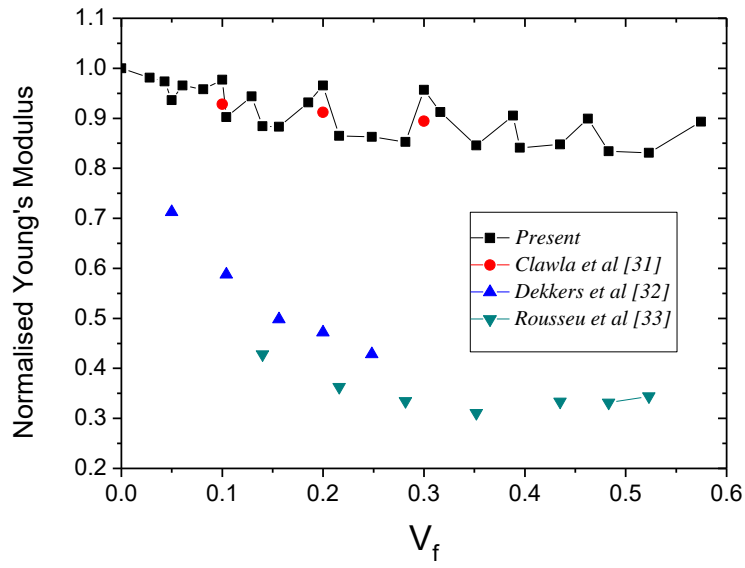
(a)
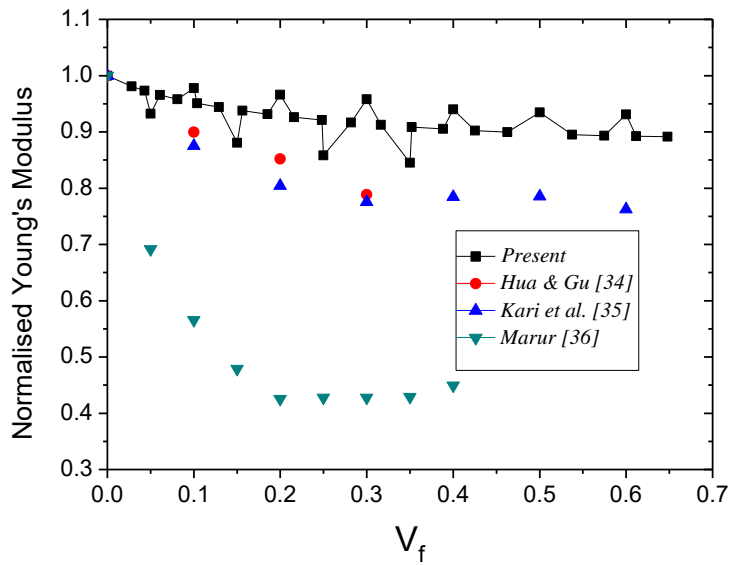


(b)

Figure 7.  Effects of filler volume fraction on the Young's modulus of interpenetrating composites when the interphase thickness is zero ($\tau = 0$ or $\tau << t$), where the Young's modulus is normalised by the Hashin and Shtrikman's upper limit.   (a) Comparison with experimental results [31-33]; (b) Comparison with simulation results [34-36].